An examination of absolute calibration of detectors and measurement of spectral radiance using correlated two-photons from parametric down-conversion.

Mark R. Ackermann
Department of Physics and Astronomy, University of New Mexico, Albuquerque NM 87131
Tel: (505) 844-1112, email: mracker@sandia.gov
(Received 22 November 1999)

Using correlated photons from parametric down-conversion, it is possible to measure the absolute quantum efficiency of photon detectors. The technique is also applicable to measuring the intrinsic absolute radiance of a photon source. This measurement allows absolute calibration of both a source and a detector without making relative measurements against externally calibrated sources or detectors. This paper examines the underlying physics of correlated photon production and parametric down-conversion and discusses applications to detector and source calibration.

PACS number(s): 42.62.Eh, 42.72-g, 42.65.Ky, 42.79.Nv

I. Introduction

For most people quantum mechanics is one of the more difficult areas of physics to understand. While its successes are most impressive, its inability to convincingly explain several basic experiments without invoking arguments of almost religious significance is distressing. Hence, the philosophical foundations of quantum mechanics remain the source of considerable controversy.

On the other hand, classical physics is easier for most people to understand as the explanations for observed phenomena can be related to common experiences. Often, quantum mechanics appears to pursue "odd theories" to explain phenomena which in many cases can be explained with semi-classical arguments. Many of the great quantum successes such as explanations of Bremsstrahlung radiation, the Lamb shift, spontaneous emission, vacuum polarization, blackbody radiation, the Raman effect, the Compton effect and the photoelectric effect all have easily understood semi-classical explanations [1]. The success of some theorists at explaining what appear to be quantum effects with semi-classical theories does little to enhance the image of quantum mechanics in the mind of nonbelievers. There are however, some processes that cannot be explained classically such as the scattering of light by light and spontaneous parametric scattering of light (SPSL).

This paper, will examine one of these phenomena with real-world applications which only have an explanation in quantum mechanics. Specifically, this paper will examine correlated photon production from parametric down conversion (PDC) and its applications to absolute calibration of both detectors and radiometric sources without comparison to externally calibrated standards.

Throughout the literature, PDC is sometimes referred to as spontaneous parametric scattering of light (SPSL) [2] and parametric fluorescence [3]. Here the phenomena will be referred to as parametric down conversion (PDC).

While PDC in a nonlinear medium can be explained with classical arguments, the spontaneous generation of photon pairs with only the presence of a pump laser, or spontaneous parametric fluorescence, is a purely quantum effect requiring quantization of the field and quantized vacuum fluctuations [4]. PDC is normally classified as a three-wave mixing nonlinear effect. However, due to vacuum fluctuations, PDC can occur with only a single input beam. The other two beams result from the PDC process itself. The pump beam spontaneously decays into signal and idler beams at wavelengths longer than the pump provided energy and momentum are conserved in the crystal. The designations of 'signal' and 'idler' are historical and date to when parametric amplification was first demonstrated in microwave cavities.

Spontaneous PDC results in the production of paired photons, one in the signal beam and one in the idler. The photons are correlated with almost absolute certainty, hence, the presence of one indicates the existence of the other [2]. This property makes possible a variety of unique applications such as highly accurate transmission and absorption measurements of material samples [4], measuring the linear refractive index of nonlinear materials at wavelengths where strong absorption occurs [4], and the subject of this paper, absolute calibration of photon detectors [5] and radiometric sources [6].

II. Parametric Down Conversion

PDC is a three wave mixing phenomena which occurs in the presence of a $\chi^{(2)}$ non-linearity. This effect is usually seen in crystals with a second order nonlinear component to the polarizability. Under the right conditions, energy is transferred from the pump to the signal and idler beams. The 'right conditions' are known as the phase matching conditions. They require conservation of momentum and energy within the crystal. These conditions are expressed as

$$\omega_p = \omega_s + \omega_i$$

and

$$\vec{k}_p = \vec{k}_s + \vec{k}_i + \Delta\vec{k} \ ,$$

where ω and **k** are the frequency and wave vector of the various beams within the crystal. The subscript **p** signifies the pump, **s** the signal and **i** the idler. Δ**k** accounts for any

mismatch in phase among the three beams. Ideally $\Delta\mathbf{k}$ is zero. Non-zero values arise from the finite length of the nonlinear crystal. The phase matching conditions are rather stringent constraints and are difficult to meet. In general, they can only be met in a nonlinear crystal.

To understand PDC, we turn to quantum mechanics and follow a derivation along the lines of that published by Louisell and Yariv [7]. While it is possible to understand most of the physics from a classical derivation, the classical result cannot explain the phenomena of spontaneous parametric fluorescence. The quantum development requires quantization of the electromagnetic field and the vacuum. A review of field quantization can be found in texts such as [8]. The goal of the present development is to obtain time-dependent equations for the creation and annihilation operators $\hat{a}_s^+(t)$, $\hat{a}_s(t)$, $\hat{a}_i^+(t)$ and $\hat{a}_i(t)$ of the parametric modes ω_s and ω_i. (Note: The notation $\hat{a}_s^+(t)$ is used for the Hermitian conjugate of $\hat{a}_s(t)$.)

For the present development, we use a formalism which couples a classical pump with two quantum modes of the field, the signal and the idler. This development is sufficient to understand PDC. However, to fully understand the dynamics of the process and obtain a theoretical understanding of how closely in time the paired photons are created, a multi-mode or contimuum of modes development as presented in [9] is necessary.

Usual development begins by considering the EM fields in a cavity of finite volume. Later this volume is extended to fit the nature of the problem. For this presentation, the initial volume can be that of the nonlinear crystal. While not specifically presented, rather than extending the volume to include more field modes, it is appropriate to apply cyclic boundary conditions.

Beginning with a cavity volume, the fields are given as

$$\vec{E} = -\frac{1}{c}\frac{\partial A}{\partial t} \quad \text{and} \quad \vec{H} = \nabla \times A\,, \tag{1}$$

where A is the field vector potential A(**r**,t) and **r** is the position vector. Classically, the vector potential is expanded as a set of cavity modes as

$$A(r,t) = \sum_k q_k(t)u_k(r)\,, \tag{2}$$

where $q_k(t)$ and $\mathbf{u}_k(\mathbf{r})$ satisfy

$$\frac{d^2 q_k}{dt^2} + \omega_k{}^2 q_k = 0 \quad \text{and} \quad \nabla\times\nabla\times u_k = \left(\frac{\omega_k}{c}\right)^2 u_k\,.$$

Usual boundary conditions require that tangential components of $\mathbf{u}_k$ and normal components of $\nabla\times u_k$ vanish. Normalization requires

$$\int_V u_k u_{k'} dV = 4\pi c^2 \delta_{kk'}\,.$$

The free-field Hamiltonian is given as

$$H_o = \tfrac{1}{8\pi}\int_V (\vec{E}^2 + \vec{H}^2)dV\,.$$

Using $d\mathbf{q}_k/dt = \mathbf{p}_k$, applying boundary conditions and some vector identities, we can rewrite the Hamiltonian as

$$H_o = \tfrac{1}{2}\sum_k (p_k^2 + \omega_k^2 q_k^2)\,. \tag{3}$$

Next we quantize the free-field Hamiltonian by replacing the quantities $\mathbf{p}_k$ and $\mathbf{q}_k$ with Hermitian operators $\hat{p}_k$ and $\hat{q}_k$ which satisfy the commutation relations

$$[\hat{p}_k, \hat{p}_{k'}] = 0 = [\hat{q}_k, \hat{q}_{k'}] \quad \text{and} \quad [\hat{q}_k, \hat{p}_{k'}] = i\hbar\delta_{kk'}\,.$$

$\hat{p}_k$ and $\hat{q}_k$ are in-turn expressed in terms of the non-Hermitian operators $\hat{a}_k$ and $\hat{a}_k^+$ as

$$\hat{q}_k(t) = \sqrt{(\hbar/2\omega_k)}(\hat{a}_k^+(t) + \hat{a}_k(t))\,, \tag{4a}$$

$$\hat{p}_k(t) = i\sqrt{(\hbar\omega_k/2)}(\hat{a}_k^+(t) - \hat{a}_k(t))\,, \tag{4b}$$

and the commutation relations for $\hat{a}_k$ and $\hat{a}_k^+$ are found to be

$$[\hat{a}_k, \hat{a}_{k'}^+] = \delta_{kk'}\,,$$
$$[\hat{a}_k, \hat{a}_k] = 0 = [\hat{a}_k^+, \hat{a}_{k'}^+]\,.$$

Then the free-field Hamiltonian (3) can be rewritten as

$$\hat{H}_o = \sum_k \hbar\omega_k(\hat{a}_k^+\hat{a}_k + \tfrac{1}{2})\,.$$

$\hat{a}_k$ and $\hat{a}_k^+$ are the usual Heisenberg annihilation and creation operators respectively. They satisfy the usual equations

$$\hat{a}_k^+ \hat{a}_k \left| n_k \right\rangle = n_k \left| n_k \right\rangle ,$$
$$\hat{a}_k^+ \left| n_k \right\rangle = \sqrt{n_k + 1} \left| n_k + 1 \right\rangle ,$$
$$\hat{a}_k \left| n_k \right\rangle = \sqrt{n_k} \left| n_k - 1 \right\rangle ,$$

where n_k is the number of photons in the state $\left| n_k \right\rangle$ and $\hat{a}_k^+ \hat{a}_k = \hat{n}_k$, the number operator. As $\hat{a}_k$, $\hat{a}_k^+$ and $\hat{H}_o$ are all Heisenberg operators, their equations of motion are

$$i\hbar \tfrac{d}{dt} \hat{a}_k = [\hat{a}_k, \hat{H}_o] = \hbar \omega_k \hat{a}_k , \quad (5a)$$
$$i\hbar \tfrac{d}{dt} \hat{a}_k^+ = [\hat{a}_k^+, \hat{H}_o] = -\hbar \omega_k \hat{a}_k^+ , \quad (5b)$$

with solutions

$$\hat{a}_k(t) = \hat{a}_{ko} e^{-i\omega_k t} \text{ and } \hat{a}_k^+(t) = \hat{a}_{ko}^+ e^{i\omega_k t} , \quad (5c)$$

indicating as expected for a free-field Hamiltonian, the total number of photons in mode k is constant in time.

To enable coupling between various modes of the field, we introduce a nonlinear relative dielectric constant of the form

$$\varepsilon(r,t) = 1 + \varepsilon'(r,t) = 1 + \Delta\varepsilon \cos(\omega t + \varphi) f(r) , \quad (6)$$

where f(**r**) is yet to be specified. We assume Δε is weak and φ is some arbitrary phase.

With Eq. (6), the Hamiltonian now has the form of

$$\hat{H} = \hat{H}_o + \hat{H}' ,$$

where

$$\hat{H}' = \tfrac{1}{8\pi} \int_V \varepsilon'(r,t) \vec{E}^2 dV .$$

This interaction Hamiltonian is more easily recognized in the form

$$\hat{H}' = \tfrac{1}{8\pi} \int_V \chi^{(2)}_{pkk'} \vec{E}_k \vec{E}_{k'} dV .$$

Given Eq. (4) and a little math, the equation for $\hat{H}'$ is found to be

$$\hat{H}'(t) = -\hbar \cos(\omega t + \varphi) \sum_{k,k'} C_{k,k'} (\hat{a}_k^+ - \hat{a}_k)(\hat{a}_{k'}^+ - \hat{a}_{k'}) , \quad (7)$$

where the coupling coefficients $C_{k,k'}$ are given as

$$C_{k,k'} = \frac{\Delta\varepsilon}{16\pi c^2} \sqrt{\omega_k \omega_{k'}} \int_V f(r) u_k u_{k'} dV . \quad (8)$$

With the nonlinear relative dielectric constant, we return to Eqs. (5) and use the complete Hamiltonian to calculate equations of motion for $\hat{a}_k$ and $\hat{a}_k^+$ as

$$\frac{d\hat{a}_k^+}{dt} = i\omega_k \hat{a}_k^+ + i[e^{i(\omega t + \varphi)} + e^{-i(\omega t + \varphi)}] \sum_{k'} C_{k,k'} (\hat{a}_{k'}^+ - \hat{a}_{k'}) \quad (9)$$

and the equation for $\hat{a}_k$ is the Hermitian conjugate of (9).

Equation (9) and its Hermitian conjugate will couple modes of frequency ω, ω_k and $\omega_{k'}$ if the coupling coefficient, $C_{k,k'}$ is nonzero for some k and k'. This requires the unspecified function f(**r**) be nonzero over some region. In general, most choices of f(**r**) will result in coupling an infinite number of modes. Classical derivations are able to limit the coupling to only a few modes. The quantum approach however, requires careful selection of the pump frequency to limit coupling to only two modes.

In the absence of mode coupling, Eq. (5c) gives the time dependence of $\hat{a}_k$ and $\hat{a}_k^+$. Combining with Eq. (9) and its Hermitian conjugate and employing first order perturbation theory, we see that

$$\left(\frac{d\hat{a}_k^+}{dt} \right)_{\hat{H}'} = i[e^{i(\omega t + \varphi)} + e^{-i(\omega t + \varphi)}] \sum_{k'} C_{k,k'} [\hat{a}_{k'o}^+ e^{i\omega_{k'} t} - \hat{a}_{k'} e^{-i\omega_{k'} t}]$$

Notice that conditions on ω and $\omega_{k'}$ are such that they give rise to a time dependence for $\hat{a}_k^+$ of $(i\omega_k t)$. This places restrictions on ω and $\omega_{k'}$. That is, the time dependence of $\hat{a}_k^+$ requires that the coupled modes result in changes in $\hat{a}_k^+$ synchronous with the free-field behavior. Much like in the rotating wave approximation, terms which are not synchronous result in a rapid beating of one state against another which averages to zero on any relevant time scale.

With the above development and restrictions, we have two modes coupled by a pump beam at frequency ω. We shall now refer to these modes as the signal and idler at frequencies ω_s and ω_i, such that $\omega = \omega_s + \omega_i$. Then considering only these modes, Eqs. (7,9) are rewritten as

$$\hat{H}'(t) = -\hbar C [\hat{a}_s^+ \hat{a}_i^+ e^{-i(\omega t + \varphi)} + \hat{a}_s \hat{a}_i e^{i(\omega t + \varphi)}]$$

and

$$\tfrac{d}{dt}\hat{a}_s^+ = i\omega_s\hat{a}_s^+ - iCe^{i(\omega t+\varphi)}\hat{a}_i\,, \qquad (10a)$$

$$\tfrac{d}{dt}\hat{a}_i^+ = i\omega_i\hat{a}_i^+ - iCe^{i(\omega t+\varphi)}\hat{a}_s \qquad (10b)$$

plus their Hermitian conjugates. Here C is the coupling coefficient for the two modes in question. These equations show signal and idler photons being created or annihilated in pairs at the expense of a pump photon. This is the parametric down conversion process. In this mode, the crystal also functions as an amplifier and hence, such applications of crystals are often given the general name 'optical parametric amplifiers' or OPAs. The PDC effect has other modes of operation which are equally interesting but not the subject of this paper. One such mode is when $\omega = \omega_s - \omega_i$, then the effect functions as a frequency converter.

Notice that from Eq. (10), we see that

$$\tfrac{d}{dt}(\hat{a}_s^+\hat{a}_s) = \tfrac{d}{dt}(\hat{a}_i^+\hat{a}_i)\,. \qquad (11)$$

These are known as the Manley-Rowe relations [5]. As the number operator is defined as $\hat{n}_s = \hat{a}_s^+\hat{a}_s$ (with the identical form for the idler), it is clear from Eq. (11) that the number of signal photons exactly equals the number of idler photons. This is critical to the use of PDC for absolute calibration of detectors. Signal and idler photons are exactly correlated. One implies the presence of the other.

The solutions for Eqs. (10) are found to be

$$\hat{a}_i(t) = e^{-i\omega_i t}(\hat{a}_{io}\cosh(Ct) + ie^{-i\varphi}\hat{a}_{so}^+\sinh(Ct))\,, \qquad (12a)$$

$$\hat{a}_s^+(t) = e^{i\omega_s t}(\hat{a}_{so}^+\cosh(Ct) - ie^{i\varphi}\hat{a}_{io}\sinh(Ct))\,, \qquad (12b)$$

plus their Hermitian conjugates. These are similar to equations presented by other authors [5]. Recall that C is the coupling coefficient for the two modes. Later we will see that C is actually the exponential amplification coefficient. From Eqs. (12), it follows that

$$\hat{n}_i(t) = \hat{n}_{io}\cosh^2(Ct) + (1+\hat{n}_{so})\sinh^2(Ct) + \tfrac{1}{2}i\sinh(2Ct)[\hat{a}_{io}^+\hat{a}_{so}^+e^{-i\varphi} - \hat{a}_{io}\hat{a}_{so}e^{i\varphi}]\,, \qquad (13a)$$

$$\hat{n}_s(t) = \hat{n}_{so}\cosh^2(Ct) + (1+\hat{n}_{io})\sinh^2(Ct) + \tfrac{1}{2}i\sinh(2Ct)[\hat{a}_{io}^+\hat{a}_{so}^+e^{-i\varphi} - \hat{a}_{io}\hat{a}_{so}e^{i\varphi}]\,. \qquad (13b)$$

Equations (13) are different from their classical equivalents. The factor of "**1**" indicates that even when the initial number of signal and idler photons are zero ($\hat{n}_{io} = \hat{n}_{so} = 0$), we still get equal numbers of signal and idler photons in the output. This is the result of spontaneous parametric down conversion. It results from quantum fluctuations of the vacuum and represents the equivalent signal and idler inputs of one photon per mode. This effect makes absolute calibration of detector quantum efficiency and source spectral radiance possible. The vacuum fluctuations seed the PDC process and result in paired photon outputs even with no signal or idler inputs.

III. Absolute Calibration

It is often said that there are two fundamental problems in radiometry, having calibrated detectors to measure a source and having a calibrated source to measure the performance of detectors. Conventional approaches usually involve one of two types of measurements. Either the detector is used to record the signature of a known calibration source, or the measurement with the unknown detector is compared to one made with a previously calibrated detector. Either way, the result is a measurement calibrated against a chain of measurements leading back to some primary calibration standard. Calibration of the primary standard usually relies on a well controlled process where a calorimeter is used to record some energy input. These techniques always involve a change entropy. No matter how precisely such procedures are performed, there are always sources of error.

Calibration using paired photons from PDC is somewhat unique. The techniques are relatively new and somewhat unknown in the world of radiometry. First, the process is exceedingly simple. Calibrations do not require comparison of measurements to a standard or accounting for various system efficiencies. Second, the process is absolute and self consistent. Two detectors of unknown quantum efficiency are used to calibrate one another. The calibration is absolute because it is based on one very simple fundamental physical process, PDC. Third, even with an unknown detector, it is possible to absolutely calibrate the spectral radiance of an unknown source without comparison to another detector or a standard. Finally, it is possible to use detectors and sources which operate in different parts of the spectrum to calibrate one another (UV to thermal IR depending on the crystal and phase matching conditions).

Because the process is simple and robust, anyone with a small laser and the right nonlinear crystal can have absolute calibration. There is no need for expensive standards or sending sensors out to be externally calibrated.

A. Absolute Detector Calibration

Absolute calibration of photon detectors relies on the absolute correlation of paired photons from the spontaneous PDC effect. The goal is to calibrate the quantum efficiency of some detector within a given range of wavelengths centered on λ_s or λ_i, the signal or idler wavelengths. All that

is required is a PDC system generating photons at the desired wavelength and a detector sensitive at the idler wavelength. Neither detector need be calibrated.

In theory, it is possible to absolutely calibrate both detectors at the same time. In practice however, due to issues associated with experiment setup, one detector is used to precisely calibrate the other. Which detector gets calibrated is arbitrary and only depends on the setup. The roles can be interchanged with a suitable change in optical components.

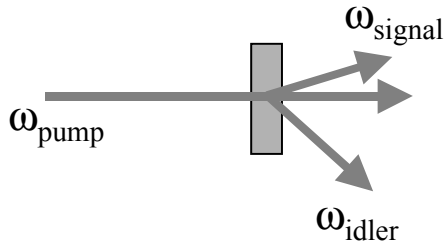

FIG. 1. An illustration of the various beams in spontaneous PDC. The geometry shows one possible arrangement obeying the phase matching conditions. Notice that the signal and idler beams are oriented at different angles from the pump. Photons from the two beams are perfectly correlated.

First we look at the basic procedure where both detectors are calibrated. This will show the simple nature of the basic technique. Then we discuss the more practical case where both detectors are used but only one results in an absolute calibration. The technique is along the lines of that published in numerous journal articles [2,6,10-13].

Consider a situation where the signal and idler detectors exactly intercept signal and idler photons with conjugate matched spectral bandwidths. If in a given time, N photons strike the signal detector, then in the same time exactly N photons will strike the idler detector.

If the quantum efficiency of the signal and idler detectors are η_s and η_i respectively, then the number of counts registered by each detector is given as

$$N_s = \eta_s N \quad \text{and} \quad N_i = \eta_i N, \tag{14}$$

and the coincident count rate is given as

$$N_c = \eta_i \eta_s N. \tag{15}$$

From Eqs. (14-15), the absolute quantum efficiency of each detector is

$$\eta_i = N_c / N_s \quad \text{and} \quad \eta_s = N_c / N_i . \tag{16}$$

Theoretically, this is all that is required to absolutely calibrate two detectors. Collect counts for the single detectors and the coincident events and form simple ratios. The calibration is absolute, there are no constants or curve fit parameters. However, the procedure is a bit more difficult in practice making it possible to calibrate only one detector at a time.

The difficulty in simultaneously calibrating two detectors has to do with production of the paired photons. When a photon pair exits the crystal, the geometry is not quite as shown in Fig. 1. The actual geometry is three dimensional. The photons emerge from the crystal in cones centered on the pump beam axis. A single pair of photons will emerge along conjugate vectors, but subsequent pairs of conjugate photon vectors can be located anywhere around the cone.

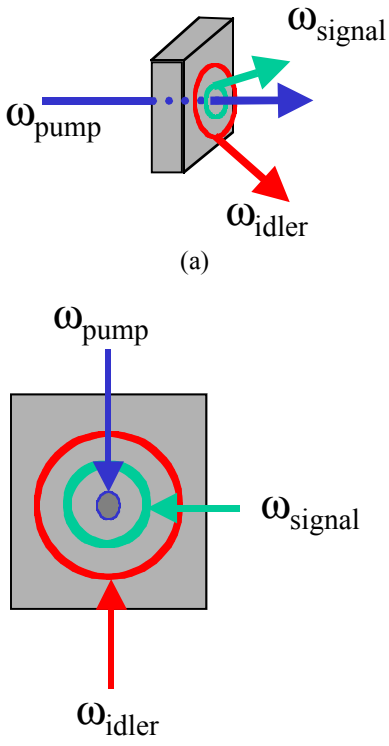

FIG. 2. (a) Pairs of photons emerge from the crystal in cones along conjugate vectors which can be oriented anywhere around cones centered on the pump beam. (b) An end view of the colored cones emerging from the crystal. The colors here are notional. The pump has the shortest wavelength while the idler has the longest. The width of the cones depends on the phase matching properties of the crystal.

The width of the cones depends on how precisely the phase matching conditions are met within the crystal and what spectral bandpass a given phase matching geometry will allow. When placing detectors to intercept signal and idler beams, they need to be some distance from the crystal to minimize the detection of out-of-band photons. Generally

this is accomplished with narrow bandpass filters and precisely placed apertures. However, the quantum efficiency measurements resulting from Eqs. (14-16) yield the total quantum efficiency. Fresnel losses at filters, miss aligned or miss centered apertures, and miss positioned detectors all result in lowering the number of photons a given detector sees. Thus if one is not careful, the quantum efficiency calculated, while absolutely correct for the experimental setup, will be of limited accuracy for the individual detector.

The solution to this problem is to calibrate only one detector at a time. That detector has a broad entrance aperture with no filters to ensure it collects all photons conjugate to the second. The second detector has a small entrance aperture very precisely defining the center wavelength and bandpass the detector sees. A narrow bandpass filter is also used to eliminate stray photons from scattering within the crystal. While this arrangement reduces the counts detected by the second detector, this does not affect the calibration of the first detector.

If the detector to be calibrated is the signal detector, then the idler detector should have the narrow entrance aperture and narrow bandpass filter. Again, individual detector and coincidence counts are recorded and the quantum efficiency of the signal detector is given as

$$\eta_s = N_c / N_i = \eta_s \eta_i N \; / \; \eta_i N. \qquad (17)$$

As shown in Eq. (17), the filters and apertures which reduce the apparent quantum efficiency of the idler detector cancel out in the equation. We are left with an absolutely calibrated signal detector.

There is one other problem which can arise while using this technique for detector calibration. That is the problem of coincidence detection. We know that the paired photons are produced almost simultaneously. Early experiments suggested the photons were produced within a few nanoseconds of one another [14], however, more recent measurements suggest that the time delay is on the order of 100ps [15]. This latter value is in excellent agreement with a full multi-mode theoretical treatment by Hong and Mandel [9].

If the time gate used for the coincidence circuitry has a characteristic width of τ_g, then we will have a finite rate of coincident counts from random detection overlap given as

$$b_c = N_s N_i \tau_g.$$

If this background coincidence rate is to have negligible effect, then it is necessary that $N_c >> b_c$. This suggests that

$$N \tau_g << 1,$$

which effectively limits the photon arrival rate at either detector. This says that we must keep the intensities and the count rates low.

B. Absolute Source Calibration

There are times when one needs to calibrate a source rather than a detector. A technique similar to that used for detector calibration can be used to measure the absolute spectral radiance of a source. The technique results in a measure of source brightness in the fundamental quantum unit of *photons per mode*. One research team refers to this unit of measure as the ***plank*** [16]. However, there remains confusion in the literature as to exactly what constitutes one photon per mode [6,16-18].

Photons per mode is a measure of spectral radiance although Klyshko [16] prefers to call this the spectral concentration of radiance as it has units of W/m^2-μm-sr. The two most common values given for one photon per mode are

$$hc/\lambda^3 \quad \text{and} \quad hc^2/\lambda^5.$$

Both are correct but the usage depends on how the spectral interval is specified. When the spectral interval is measured in units of wavelength, the spectral radiance equals

$$\text{one photon per mode} = hc^2/\lambda^5 \quad (\text{W/m}^3\text{-s-sr}).$$

When the spectral interval is measured in units of frequency, the spectral radiance equals

$$\text{one photon per mode} = hc/\lambda^3 \quad (\text{W/m}^2\text{-sr}).$$

The units (per sr) do not come about from the constants themselves. It is necessary to remember that the spectral radiance is measured over some collection solid angle, or radiated into some solid angle. Klyshko [16] notes that at λ=1 micron, one photon per mode is roughly 0.6 W/angstrom-cm^2-sr.

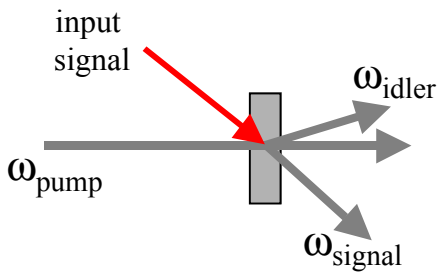

FIG. 3. The basic setup for stimulated PDC. Notice that the signal and idler designations have been reversed. Their order does not matter but it made sense to keep the PDC signal associated with the input signal. Notice also that the

PDC process generates the idler wave. Since the idler photons are conjugate pairs with the signal photons, the idler beam contains all the information about the IR source but at a visible wavelength.

To calibrate the absolute spectral radiance of a source, we again use paired photons from PDC. We also make two separate measurements and ratio their results to arrive at the desired quantity. However, the overall approach is somewhat different as source calibration relies on the stimulated PDC process.

Stimulated PDC is another process which occurs in nonlinear crystals. When a weak signal is brought in such that it is aligned with the internal phase matched signal beam in both wavelength and direction, it stimulates the PDC process resulting in paired signal and idler photons. The idler beam is at a different wavelength.

To see how the input signal beam affects the number of photons in the signal and idler beams, we return to Eqs. (13). $\hat{n}_{io}$ represents the initial number of idler photons which is zero. $\hat{n}_{so}$ is the initial number of signal photons. This is the number of photons input into the crystal from the IR source to stimulate the PDC process. It is an unknown at this time. Then, dropping the phase terms as we are only concerned with the time average values, we find that Eqs. (13) can be rewritten as

$$\hat{n}_{io}(t) = (1+\hat{n}_{so})\sinh^2(Ct)\,, \qquad (18a)$$

$$\hat{n}_{so}(t) = \hat{n}_{so}\cosh^2(Ct) + (1)\sinh^2(Ct)\,. \qquad (18b)$$

Notice the term $(1+\hat{n}_{so})$ in Eq. (18a). The **1** represents the one photon per mode contribution of vacuum fluctuations. In the last term of Eq. (18b) we see another **1**. This was left in the equation to emphasize its origins.

Assume that the unknown source radiates somewhere in the SWIR and that the pump laser, crystal and phase matching conditions are selected such that the idler beam will be in the visible (or near visible – still in the sensitive detection range for silicon). To make an absolute radiometric calibration of the source, we place our detector on the idler beam and make two measurements: one with the source signal entering the crystal, the other with it blocked. If we define $\hat{n}_{iout}(ON)$ as the idler output when the source signal is allowed to enter the crystal, and $\hat{n}_{iout}(OFF)$ as the idler output when the source signal is blocked, we find that their ratio

$$\frac{\hat{n}_{iout}(ON)}{\hat{n}_{iout}(OFF)} = \frac{[1+\hat{n}_{so}]\sinh^2(Ct)}{[1]\sinh^2(Ct)} = 1+\hat{n}_{so}\,.$$

The ratio of these two measurements gives a spectral radiance of $(1+\hat{n}_{so})$ photons per mode. Then, the absolute spectral radiance of the source is

$$\frac{\hat{n}_{iout}(ON)}{\hat{n}_{iout}(OFF)} - 1 = \hat{n}_{so} \text{ photons per mode.}$$

Thus, we can use PDC to exactly calibrate an unknown thermal source. The measurement does not require a calibrated detector. The source black body temperature can be calculated from

$$T(^\circ K) = \frac{\hbar\omega_k}{k_B \ln(1+1/\hat{n}_{so})}\,,$$

where k_B is the Boltzman constant.

C. Results of Published Experiments

Aside from being interesting physics, the theory of detector and source calibration also has practical applications. Results of a number of experiments appear in the literature but it is not the focus of this paper to simply recount these. Mostly what is learned from reviewing published experiments are the details of the laboratory setup. While based on simple physical principles, the experiments are not trivial to implement.

In one experiment, Migdall et al. [6] set out to measure the spectral radiance of a source at 3.415 and 4.722μm. They used a 457.9nm Argon ion laser as the pump and a $LiIO_3$ crystal cut with the optic axis inclined 33.6° from surface normal. The conjugate photon pairs were at 0.5288 and 3.415μm and 0.5065 and 4.722μm. Their setup was defined as Type 1, with the pump being an extraordinary ray and both the signal and idler being ordinary rays with the same polarization. The radiance was measured along the visible idler beam using a silicon avalanche photodiode. Results of the PDC measurement were compared with results from a detector calibrated by the National Institute of Standards (NIST). The two measurements agreed to within 3%. This is excellent agreement for two such measurements.

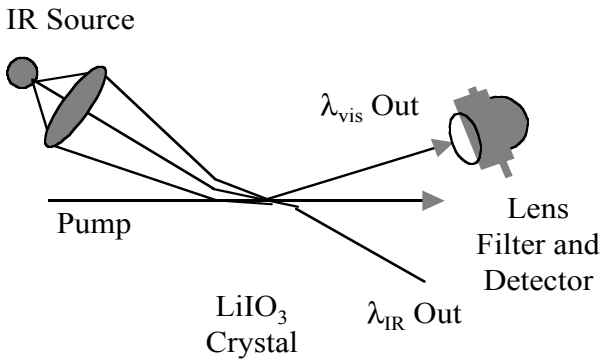

FIG. 4. Experimental setup used by Migdall et al. [6] for absolute source calibration.

One question left open by the Migdall experiment is that of which measurement contained the error. It is most likely that both measurements had some error as techniques for the PDC approach are still being refined. Unfortunately it is being reported by some that the NIST experiments demonstrated the PDC technique to be within 3% of absolute. It is likely in the future that NIST will use the PDC technique as the new absolute standard.

Table 1. Results of source calibration experiment [6].

In-Band Spectral Radiance (photons/mode)	λ=3.415μm	λ=4.772μm
Conventional Measurement	0.6057 +/- 0.0130	1.6455 +/- 0.0322
Correlated Photon Measurement	0.5947 +/- 0.0117	1.6575 +/- 0.0186

In another experiment, Migdall et al. [5] demonstrated the PDC technique for calibrating a photo multiplier tube at four separate wavelengths. In this experiment, the second detector was an avalanche mode silicon photodiode. The pump beam was from an Argon ion laser at 351.1nm. The nonlinear crystal was KDP with the optic axis inclined 52° to the surface normal of the input face. The four conjugate wavelength pairs (signal and idler) selected for the calibration were

APD	702nm	608nm	633nm	788.6nm
PMT	702nm	831nm	789nm	633.2nm

Note that the first set of wavelengths constitute the degenerate point where signal and idler are identical. The polarization was Type 1. Comparison of the PDC calibrations with calibrations against conventional NIST standards demonstrated agreement to within 3.13% at one wavelength and within less than 1% at the other three wavelengths. These results are shown in Fig. 5.

What is important to note in these experiments is that while detector and source calibration experiments are really in their early stages, they already compare favorably with calibrations against precision standards at NIST. The reason the two experiments by Migdall et al. were discussed here is that they were conducted at NIST where the research teams have direct access to primary calibration standards rather than equipment with a second, third or fourth generation calibration pedigree. Standards and calibration are of course, primary functions of NIST. They are working with PDC calibration techniques to assess their suitability for replacing existing primary standards. The other important point is that these calibrations did not involve any process with a large change in entropy. The experiments are conceptually simple. Details of these and other experiments are available in some of the references [2,5-6,9-13,16-18].

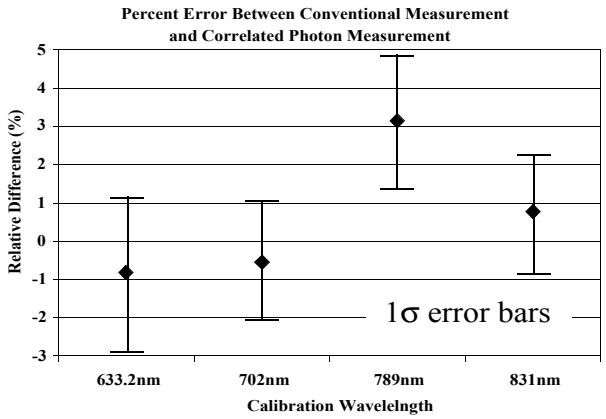

FIG. 5. Results of the absolute detector calibration experiment by Migdall et al. [5].

IV. Other Applications of PDC

The parametric down conversion process has a number of other applications which include parametric amplification, frequency conversion, a parametric oscillator, a precise source of temporally correlated photons and a source of non-classical squeezed-state light. Even a brief treatment of all these applications is beyond the scope of this paper. However, optical parametric amplification is sufficiently similar to absolute detector calibration that it warrants a brief discussion.

Equations (12-13) are a representation of the equations for the parametric amplification process. If we are concerned with the time averaged number of photons resulting on both the signal and idler branches for the general PDC effect, Eqs. (13) become

$$\overline{n}_i = \overline{n}_{io}\cosh^2(C\tau) + (1+\overline{n}_{so})\sinh^2(C\tau), \quad (19a)$$

$$\overline{n}_s = \overline{n}_{so}\cosh^2(C\tau) + (1+\overline{n}_{io})\sinh^2(C\tau)\,. \quad (19b)$$

The time dependence has been replaced with τ, the interaction time for photons crossing the region of the crystal where three wave mixing occurs. We have also changed from the operator notation, $\hat{n}$, to an average number notation, $\overline{n}$. Recall that C was the coupling coefficient between the modes. From Eqs. (1-2,8) we see that C is proportional to the square of the total electric field within the crystal. Hence, C is the gain coefficient. For any reasonable value of C, the $\cosh^2$ and $\sinh^2$ arguments reduce to $e^{2C\tau}$. We shall define this quantity as the gain G, where

$$G = e^{2C\tau}\,. \quad (20)$$

In a general application, the optical parametric amplifier (OPA) will have pump and signal inputs, much like shown in Fig. 3. Hence, the input conditions will be $n_{io} = 0$ and $n_{so} = P_{so}/\hbar\omega_s$ where P_{so} is the power of the input signal. This assumes the input signal is quasi-monochromatic which is required for the phase matching conditions. Combining Eqs. (19-20), we find the expected outputs from the signal and idler beams as

$$\overline{n}_i = (1+\overline{n}_{so})G\,, \quad (21a)$$

$$\overline{n}_s = (1+\overline{n}_{so})G\,. \quad (21b)$$

To be more precise, since this is a stimulated emission effect, Eq. (21b) should be written as

$$\overline{n}_s = (1+\overline{n}_{so})G + \overline{n}_{so} = \overline{n}_{so}(1+G) + G\,.$$

When G is not overwhelming, depletion of pump energy is not an issue and these equations are appropriate. When the gain is very high, depletion of the pump must be considered and the development of Brunner [4] should be followed. For small input signals, gains on the order of 10^4 to 10^5 are not uncommon [19].

One application of optical parametric amplification is to imagery. It is possible to inject an image into the OPA as the input signal. When overlapped with a strong pump, an amplified image is produced along both signal and idler beams.

An OPA has significant advantages over other amplifier techniques. When combined with a sub-nanosecond pulsed pump laser, the OPA allows one to achieve precise time gating and frequency selection with significant optical gain and frequency agility. In a recently published series of experiments, Cameron [19] applied an OPA to a LIDAR system and demonstrated the ability to form optical images of targets obscured by dense clouds. The OPA provided both precise time gating for scatter rejection as well as amplification to boost the weak return signal.

V. Summary

This paper has briefly discussed some of the physics of paired photon production from parametric down conversion and its applications to the absolute calibration of sources and detectors. Conventional calibrations involve either relating one measurement to more basic physics in yet another measurement, or comparison of the measurement in question against one made with a "calibrated" source or detector. Such approaches require one to trust the calibration given.

In contrast, the PDC effect allows absolute calibration of both sources and detectors. With relatively basic optical laboratory equipment, it is possible to use the PDC effect to absolutely calibrate both detector quantum efficiency and the absolute spectral radiance of a thermal photon source. The calibration is based on fundamental physical processes. There are no conversion coefficients, fudge factors or assumptions that part of some measurement contains only a small error. For either type of calibration, one simply takes the ratio of two different photon counting (or intensity measuring) events and has the answer.

Acknowledgements

The author wishes to acknowledge the time and effort invested by Dr. Stewart M. Cameron and Dr. David E. Bliss of Sandia National Laboratories in helping with discussions of the parametric down conversion processes.

References

[1] R. Kidd, J. Ardini, A. Anton, Am J Phys, **57**, 27 (1989).
[2] A. N. Penin, A. V. Sergienko, Appl Opt, **30**, 3582 (1991).
[3] D. N. Klyshko, Sov Phys JETP, **28**, 522 (1969).
[4] W. Brunner, H. Paul, Progress in Optics XV (North-Holland, 1977).
[5] A. L. Migdall, R. U. Datla, A. Sergienko, J. S. Orszak, Y. H. Shih, Metrologia, **32**, 479 (1996).
[6] A. Migdall, R. Datla, A. Sergienko, J. S. Orszak, Y. H. Shih, Appl Opt, **37**, 3455 (1998)
[7] W. H. Louisell, A. Yariv, Phys Rev, **124**, 1646 (1961).
[8] P. Meystre, M. Sargent III, Elements of Quantum Optics (Springer-Verlag, 1990).
[9] C. K. Hong, L. Mandel, Phys Rev A, **31**, 2409 (1985).
[10] P. G. Kwiat, A. M. Steinberg, R. Y. Chiao, P. H. Eberhard, M. D. Petroff, Appl Opt, **33**, 1844 (1994).

[11] V. M. Ginzberg, N. G. Keratishvilli, E. L. Korzhenevich, G. V. Lunev, A. N. Penin, V. I. Sapritsky, Opt Eng, **32**, 2911 (1993).
[12] J. G. Rarity, K. D. Ridley, P. R. Tapster, Appl Opt, **26**, 4616 (1987).
[13] A. A. Malygin, A. N. Penin, A. V. Sergienko, Sov J Phys JETP Letters, **33**, 477 (1981).
[14] D. C. Burnham, D. L. Weinberg, Phys Rev Lett, **25**, 84 (1970).
[15] S. Friberg, C. K. Hong, L. Mandel, Phys Rev Lett, **54**, 2011 (1985).
[16] D. N. Klyshko, A. N. Penin, Sov Phys Usp., **30**, 716 (1987).
[17] G. Kh. Kitaeva, A. N. Penin, V. V. Fadeev, Yu. A. Yanait, Sov Phys Dokl, **24**, 564 (1979).
[18] E. Dauler, A. Migdall, N. Boeuf, R. U. Dalta, A. Muller, A. Sergienko, Metrologia, **35**, 295 (1998).
[19] S. M. Cameron, D. E. Bliss, R. A. Hamil, Proc IRIS Spec Grp Actv Sys, **3**, 21 (1998).